JOURNAL OF AIRCRAFT
Vol. 46, No. 6, November–December 2009

Engineering Notes

Optimization of Rotorcraft Simultaneous Noninterfering Noise Abatement Approach Procedures

H. G. Visser,* M. D. Pavel,† and S. F. Tang‡
Delft University of Technology,
2600 GB Delft, The Netherlands

DOI: 10.2514/1.39763

I. Introduction

THE concept of simultaneous noninterfering (SNI) approaches for rotorcraft is currently being explored in both Europe and the United States. The SNI concept was initially conceived in the United States to enable the integration of both fixed wing and rotorcraft into the terminal airspace system to reduce delays and increase capacity [1]. It comprises primarily specific instrument flight rules (IFR) departure and approach procedures which enable rotorcraft to operate independently from fixed-wing traffic IFR streams. Because of the much lower approach speeds of helicopters, sequencing helicopter operations into the IFR approach stream tends to result in congestion and undesirable delays. At present, helicopter operators often prefer to operate under visual flight rules to avoid complex IFR procedures, but clearly this does not provide a reliable air transport service in all weather conditions. Also, in Europe, research pertaining to SNI operations is well underway, notably in the sixth framework project OPTIMAL (Optimized Procedures and Techniques for Improvement of Approach and Landing) [2]. The main aim of the OPTIMAL project is to increase airport capacity and efficiency, while reducing the noise footprint.

A downside of the SNI concept is that new SNI routes will be located in previously unused airspace and consequently may overfly noise-sensitive communities that were not affected by traffic movements before. This, coupled with the fact that helicopter approach operations tend to be relatively noisy, indicates a clear need for optimization of the SNI routes and flight paths such as to reduce the noise impact in the affected residential communities.

Optimization of SNI approaches with respect to community noise impact was first explored by Atkins and Xue [3,4]. In [3,4], they present an optimization technique for segmented three-dimensional SNI trajectory design based on an incremental search strategy that combines a *k*-ary tree with Dijkstra's algorithm. The objective function is based on a validated rotorcraft noise model as well as terminal area population density data. Fixed-wing airspace corridors were treated as impenetrable obstacles. In this approach, a trajectory is described as a sequence of trimmed flight segments that connect initial approach and landing sites. The number of segments considered in this study remains limited (typically five or less) primarily due to the fact that the computational load increases rapidly with the number of segments. To make the approach numerically tractable, a number of simplifying assumptions were introduced. In particular, it was assumed that transitions between trim states do not appreciably affect solution cost.

The optimization of noise abatement procedures for fixed-wing aircraft has received considerably more attention. In [5], an optimization approach is presented that, similar to [3,4], relies on segmented routes. The segmented routes, optimized using a genetic algorithm, enable a specification of simple procedures that are amenable to fast online computer solutions that can be readily implemented in a guidance system. In [6–8], a noise-optimized approach and departure trajectories are computed based on a direct numerical optimization techniques that enable one to generate (piecewise) continuous optimal trajectories for a point-mass modeled fixed-wing aircraft. The numerical tool that has been used in these particular studies is called NOISHHH. The NOISHHH tool essentially combines a noise model, a dose-response relationship, an emission inventory model, a geographic information system, and a dynamic trajectory optimization algorithm. NOISHHH generates routings and flight paths for both arrivals and departures that minimize the environmental impact in the residential communities surrounding the airport, while satisfying all imposed operational and safety constraints.

The present study is aimed at extending the NOISHHH tool to permit the computation of noise-optimized SNI trajectories for rotorcraft. The extension does not only entail a modification of the dynamic vehicle model and the operational context, but also involves an adaptation of the implemented noise model. The environmentally-optimized SNI trajectories calculated with the modified version of NOISHHH are illustrated in an example scenario involving an SNI instrument approach of a Robinson R22 helicopter [9] to a helispot on runway 22 of Schiphol airport (Amsterdam) in the Netherlands.

II. Environmental Optimization

To date, a variety of noise abatement procedures has been proposed. Quite often, noise abatement procedures are designed to minimize the area impacted by high-intensity aircraft noise. Although the application of a procedure that is designed in this fashion may indeed result in a reduction in the area impacted by high-intensity noise, it is readily clear that an exposed area criterion can hardly be viewed as a metric for the true noise impact experienced by the residents in the exposed communities surrounding an airport. By basing noise abatement procedure design on environmental criteria that directly reflect the noise impact in the affected communities, it can be much better assured that air traffic is routed over less noise-sensitive areas.

In this study, a range of environmental performance criteria has been considered, including both generic criteria and site-specific criteria that depend on the actual population density distribution in the neighborhood of the considered landing site. To demonstrate a tradeoff between the various environmental criteria, a composite performance measure is considered that consists of a weighted combination of four relevant indicators:

$$J = \text{Fuel} + K_1 \cdot \text{Awakenings} + K_2 \cdot \text{Population}_{65\ \text{dB}} + K_3 \cdot \text{Area}_{65\ \text{dB}} \tag{1}$$

where Fuel is the fuel-consumed, Awakenings is the number of people within the exposed community that is expected to awake due to a single-event nighttime flyover, $\text{Population}_{65\ \text{dB}}$ is the population living within the 65 dB(A) level contour, and $\text{Area}_{65\ \text{dB}}$ is the total area enclosed within the 65 dB(A) contour (footprint). The

Presented at the 2009 AIAA Aerospace Sciences Meeting, Orlando, FL, 5–8 January 2009; received 14 July 2008; accepted for publication 10 August 2009.

*Associate Professor, Faculty of Aerospace Engineering, P.O. Box 5058. Associate Fellow AIAA.
†Assistant Professor, Faculty of Aerospace Engineering. Member AIAA.
‡Master's of Science Student, Faculty of Aerospace Engineering.

parameters K_i (≥ 0) are the user-selected weighting factors in the composite performance index. If so desired, a reference noise level different from 65 dB(A) can be selected. It is also possible to extend the performance index (1) to include multiple noise-level criteria.

The specification of an awakening-related performance index requires knowledge of the relationship between aircraft noise exposure and sleep disturbance. In NOISHHH, the dose-response relationship as proposed by the Federal Interagency Committee on Aviation Noise (FICAN) in 1997 has been implemented [6–8]. The 1997 curve, shown in Fig. 1, can be represented by the following relationship for the percentage of the exposed population expected to be awakened (%Awakenings) as a function of the exposure to single-event noise levels expressed in terms of sound exposure level:

$$\%\text{Awakenings} = 0.0087(\text{SEL} - 30)^{1.79} \tag{2}$$

where SEL is defined to be the sound exposure level (in debye) that is experienced indoors. It is noted that the proposed relationship represents a worst-case bound on the number of people likely to awake. It needs to be cautioned that the FICAN relationship has been established using data from field trials in which the population was exposed to flyovers of fixed-wing aircraft. Evidently, this sleep disturbance relationship may not necessarily be representative for helicopter flyovers.

In this study, indoor sound levels at observer locations are obtained by lowering the computed outdoor sound levels at those locations by 20.5 dB, which is a representative value for transmission loss for a typical home with the windows closed [7,8]. The methodology for calculating the outdoor noise exposure from each individual aircraft flyover that has been adopted in NOISHHH is based on the well-known integrated noise model INM [10]. By combining the % Awakenings results with the actual population density distribution in the noise-exposed residential communities, the absolute number of people likely to awake due to a flyover can be determined [6–8].

The INM has been the Federal Aviation Administration's (FAA) standard methodology for noise assessments since 1979. It has been developed through a succession of versions, currently at version 7.0. INM constitutes one of the most commonly used tools for conducting airport-related environmental impact studies in many countries around the globe. In the United States, INM is typically used for noise compatibility planning and for environmental impact statements under FAA order 1050 [11]. Because the community noise impact is based on aggregating all single events during the evaluation period (typically a year), it is readily clear that efforts to minimize the acoustic impact of each single-event flyover are of paramount importance.

Helicopter noise modeling was first introduced in INM version 6.0. In the most recent version of the NOISHHH toolset, the acoustic methodology of INM version 6.2 has been implemented [10]. In contrast to INM version 7.0, which includes a more detailed modeling of helicopter noise based on the FAA's heliport noise model (HNM), INM version 6.2 only provides partial implementation of HNM helicopters as fixed-wing aircraft. For example, INM 6.2 models a helicopter as a single omnidirectional point source and, as a consequence, it can only model symmetrical noise relative to the flight track. Although the present study still relies on the INM 6.2 methodology, implementation of the more advanced INM 7.0 helicopter noise modeling capabilities in the NOISHHH tool is envisioned for the near future.

INM uses tabulations of noise-power-distance (NPD) relationships for specific reference conditions for each aircraft or rotorcraft type considered. These give, for a specific aircraft speed, A-weighted SEL versus slant range from observer to aircraft/rotorcraft as a function of engine thrust settings. In the case of aircraft, the thrust settings are related to aircraft engine power states, but for rotorcraft, the thrust settings are related to the helicopter flight-path angles. There are three helicopter types available in INM with expanded NPD data sets. One of the types for which an extended set of NPD curves is available is the Robinson R22. This particular helicopter type has been selected in the present study.

From the set of NPD curves available for the Robinson R22 helicopter, noise curves are extracted for four different operational modes. Three curves represent approach mode for three different descent angles (3, 6, and 9 deg), and one curve represents level flyover. Further details can be found in [9]. The NPD data are used to either interpolate or extrapolate an associated noise-level value. The interpolation/extrapolation is a piecewise linear process between the flight-path angle and the base-10 logarithm of the distance.

In NOISHHH sound exposure levels are computed on observer locations that are arranged in the form of a uniform grid of points covering the residential areas in the vicinity of the approach path. The size and mesh of the grid have a significant impact on the computational burden of the iterative optimization process and must therefore be judiciously chosen for each specific case. The numerical example presented in this paper is based on an SNI approach to runway 22 of Schiphol airport. Figure 2 illustrates a typical example of such an SNI approach within the Schiphol control region (CTR), a zone operated by tower control. The selected cell size for the noise grid area shown in Fig. 2 is 1×1 km^2. Note that the observer (noise calculation) points are located at the centers of the grid cells. The grid adopted for the noise calculations is also used to define the population distribution.

III. Helicopter Performance Modeling

The NOISHHH tool does not rely on the flight-path computation methodology implemented in the INM package, but rather makes use of a simplified point-mass helicopter model in three-dimensions [12]. The calculations are performed in standard atmospheric conditions, and it is assumed that no wind is present in this study. Using an Earth-fixed system as a reference frame, the three-dimensional point-mass equations of motion can be written as

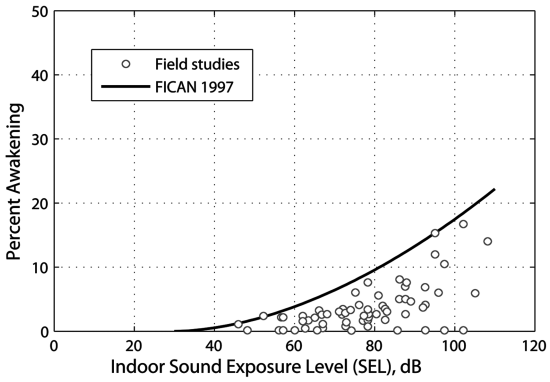

Fig. 1 FICAN proposed sleep disturbance dose-response relationship [6–8].

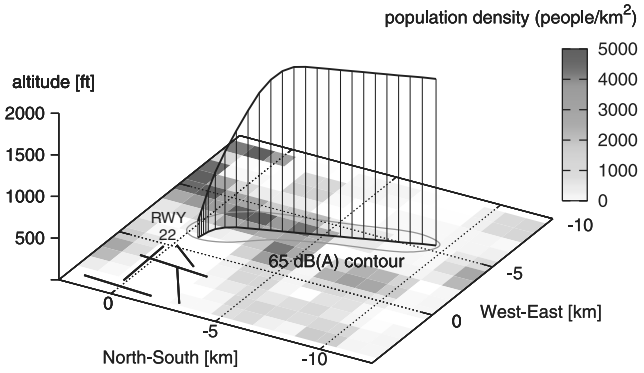

Fig. 2 Example SNI trajectory within the Schiphol CTR with underlying noise/population grid area.

$$\dot{u} = \left(C_x \rho (\Omega R)^2 \pi R^2 - f_e \frac{1}{2} \rho u V \right) \Big/ m$$
$$\dot{v} = \left(C_y \rho (\Omega R)^2 \pi R^2 - f_e \frac{1}{2} \rho v V \right) \Big/ m$$
$$\dot{w} = \left(C_z \rho (\Omega R)^2 \pi R^2 - f_e \frac{1}{2} \rho w V - mg \right) \Big/ m$$
$$\dot{x} = u \qquad \dot{y} = v \qquad \dot{h} = w \tag{3}$$

where x, y, and h are the rotorcraft position coordinates, and u, v, and w are the components of the velocity vector along the axes of the reference frame. It is assumed here that the x axis points to the north and the y axis to the west. The magnitude of the velocity vector is given by

$$V = \sqrt{u^2 + v^2 + w^2} \tag{4}$$

In Eqs. (3), f_e represents the equivalent flat plate area, Ω is the rotor angular speed, and R is the rotor radius. It is assumed that the helicopter mass m remains constant throughout the flight. Note that the variables C_x, C_y, and C_z, which are the components of the thrust coefficient vector along the axes of the reference frame, are used as the controls of the point-mass modeled rotorcraft. The thrust coefficient C_T is defined as

$$C_T = \frac{T}{\rho (\Omega R)^2 \pi R^2} \tag{5}$$

The required power coefficient C_P is obtained from the following relation [12,13]:

$$C_P = C_T \sqrt{\frac{1}{2} C_W} (K_{\text{ind}} \bar{v}_i + \bar{U}_c) + \frac{1}{8} \sigma c_d (1 + 4.65 \mu^2) \tag{6}$$

where

$$C_W = W / \rho (\Omega R)^2 \pi R^2 \tag{7}$$

is the thrust coefficient in hover, K_{ind} is the induced-power factor, $\bar{v}_i$ is the normalized induced velocity, $\bar{U}_C$ is the normalized velocity component perpendicular to the tip path plane of the rotor, σ is the solidity of the rotor, c_d is the mean profile drag coefficient of the rotor-blades, and μ is the rotor advance ratio.

Note that the main rotor power required is taken as the sum of induced power, climb power, and profile power. Although engine power should include tail rotor power and installation losses, these are secondary effects and have not been considered in NOISHHH. The power required by the helicopter P_{req} should not exceed the available power P_{avail}:

$$P_{\text{req}} = C_P \rho (\Omega R)^3 \pi R^2 \leq P_{\text{avail}} \tag{8}$$

The fuel flow is defined as the product of the specific fuel-consumption (SFC) and the required power [9]:

$$\dot{m}_{\text{fuel}} = \text{SFC} \cdot P_{\text{req}} \tag{9}$$

The R22 features an SFC value of 0.44 lb/hp/hr [9].

The controls are subjected to constraints that arise as a result of aerodynamic and structural limitations on the rotor thrust and the thrust inclination angle β:

$$\tan \beta = \frac{\sqrt{C_x^2 + C_y^2}}{C_z} \leq \tan \beta_{\max} \tag{10}$$

$$C_T = \sqrt{C_x^2 + C_y^2 + C_z^2} \leq C_{T,\max} \tag{11}$$

Note that the thrust inclination angle β is the angle between the thrust axis and the vertical axis of the reference frame.

In addition to the preceding control constraints, a variety of performance constraints, passenger comfort, and other operational constraints has been included in the SNI approach problem formulation. These constraints have been summarized in Table 1. Note that the permissible range for the flight-path angle has been set at [−9, 0 deg] to remain within the value range of the INM noise database. The constraint set also includes constraints on the range of permissible accelerations/decelerations. In this numerical example, fairly tight limits on the lateral, longitudinal, and vertical acceleration have been assumed. In particular, the imposed constraint on lateral acceleration limits the bank angle of the helicopter to just a few degrees.

One of the main reasons for imposing rather tight acceleration constraints is that the INM acoustic model does not accurately represent the external noise radiated by a maneuvering helicopter.

IV. Numerical Method

The numerical trajectory optimization method implemented in NOISHHH is the direct optimization technique of collocation with nonlinear programming (NLP). The collocation method essentially transforms an optimal control problem into an NLP formulation by discretizing the trajectory dynamics [6–8]. To this end, the time interval of an optimal trajectory solution is divided into a number of subintervals. The individual time points delimiting the subintervals are called nodes. The values of the states and the controls at the nodes are then treated as a set of NLP variables. The system differential equations are discretized and transformed into algebraic equations (implicit integration). The path and control constraints imposed in the original optimal control problem are treated as algebraic inequalities in the NLP formulation. To solve the described optimal control problem, a software package called EZopt has been used [6–8]. The collocation approach adopted in EZopt results in piecewise constant control histories and piecewise linear state histories. This

Table 1 Overview of trajectory and control constraints for approach

Constraints	Inequality
Never exceed speed	$\sqrt{u^2 + v^2 + w^2} \leq V_{\text{n.e.}}$
Maximum level speed	$\sqrt{u^2 + v^2} \leq V_{xy,\max}$
Maximum rate of descent (glide slope approach)	$-800 \text{ fpm} \leq w \leq 0$
Max/min flight-path angle	$\sin(\gamma_{\min}) \leq w / \sqrt{u^2 + v^2 + w^2} \leq 0$; $\gamma_{\min} = -9 \deg$
Max acceleration/deceleration	$\sqrt{(\dot{u})^2 + (\dot{v})^2 + (\dot{w})^2} \leq 0.05 g_0$
Maximum thrust coefficient	$\sqrt{C_x^2 + C_y^2 + C_z^2} \leq C_{T,\max}$
Maximum thrust inclination angle	$\sqrt{C_x^2 + C_y^2} \leq C_z \tan \beta_{\max}$; $\beta_{\max} = 11 \deg$
Rotor upward thrust	$C_z \geq 0$
Performance constraint	$P_{\text{avail}} \geq P_{\text{req}}$

Table 2 Summary of major results

Case no.	Primary optimization criterion	Glide slope angle, deg	Transit time, s	Fuel, kg	No. awake	Population count above 65 dB(A)	Area above 65 dB(A), km^2
1	Fuel	7.82	294	0.74	895	38,271	22.1
2	No. awake	5.13	263	0.96	477	17,932	19.1
3	Population count above 65 dB(A)	6.87	304	0.89	509	14,010	19.1
4	Area above 65 dB(A)	6.66	278	0.77	902	33,627	18.1

renders EZopt fully compatible with the discretization (segmentation) approach taken in the INM.

Generally, the accuracy of the numerical solution of the problem improves with an increasing number of subintervals, or equivalently, the number of nodes. On the other hand, increasing the number of nodes requires a larger computational effort, hence forcing a compromise between desired accuracy and computational burden. In the NOISHHH context, the adopted flight-path segmentation is primarily based on the requirements associated with the computational methodology employed in the INM model. In the present study, the overall time interval is nominally divided into 20 nonequidistant subintervals, yielding an NLP problem of 262 NLP variables and 418 nonlinear constraints.

V. Simultaneous Noninterfering Example Scenario and Procedure Design

In the example scenario, a hypothetical SNI instrument approach from the south to the helispot located on runway 22 of Schiphol airport been selected. The instrument approach procedures presently in use at Schiphol airport are optimized for fixed-wing aircraft. The geometry and speed profile of the instrument procedures introduced here are adapted to rotorcraft capabilities and are designed to avoid existing fixed-wing traffic corridors. The resulting approach procedures are suitable for rotorcraft only. At present no regulations for specific SNI rotorcraft approach procedures are in place. The procedure design conducted in this study therefore merely provides examples of possible rotorcraft procedures. The NOISHHH tool has been set up in a generic way, allowing to specify approach procedures in terms of initial and final conditions, number and type of approach procedure segments (not to be confused with INM segments), navigation system requirements, fixed-wing traffic corridor constraints, and operational limitations. To implement the various procedure segments, a so-called multiphase optimization procedure is employed in NOISHHH [6–8]. A multiphase formulation allows the implementation of different sets of constraints for different flight phases.

Figure 2 shows a typical example of a fuel-optimized approach trajectory generated with the newly developed rotorcraft-specific NOISHHH version. The trajectory comprises two approach segments only. The initial approach segment starts at a given altitude of 2000 ft, at the boundary of the control zone. However, the initial heading and speed are not specified, but have been determined in the optimization process, subject to various operational constraints. The final approach segment starts at a specified altitude of 500 ft and ends at the decision height of 200 ft. The final approach segment is assumed to be flown in a fixed direction along the localizer (heading 280 deg) and glide slope. The value of the glide slope angle is not specified a priori but is also determined in the optimization process. Also, the final speed is not specified, but selected through optimization within the operational constraints (which includes a minimum speed of 30 kts). A maximum descent rate limit of 800 fpm is imposed along the glide slope approach path. However, at the terminal point (decision altitude), the descent rate limit is reduced to 500 fpm. During the initial phase of the approach, no descent rate limitation has been enforced.

VI. Numerical Results

To investigate the noise characteristics of optimal SNI approach trajectories, a parametric investigation involving the weighting parameters in the composite noise performance index given by Eq. (1) has been conducted. All presented approach trajectories feature two segments and are initiated at an altitude of 2000 ft. The final approach phase is commenced at an altitude of 500 ft, resulting in a fairly short localizer/glide slope phase. The major results for four selected cases are summarized in Table 2. Each of the four selected cases is represented by a different set of weighting factors K_i ($i = 1$, 2, 3) in Eq. (1). The minimum-fuel formulation, with all weighting factors set to zero, is selected as a reference case (case 1). In cases 2–4, a positive value is assigned only to one of the three weighting factors. In each of these three cases, the positive weighting factor is given a fairly large value to ensure that the optimal solution is not dominated by fuel considerations.

The airspeed and altitude profiles of the optimal trajectory solutions for cases 1–4 are shown in Fig. 3. The corresponding ground tracks are shown in Fig. 4. A comparison of the ground tracks shown in Fig. 4 shows that the two solutions corresponding to a site-specific criterion, viz., the case 2 and 3 solutions, feature very similar ground tracks that circumnavigate the most densely populated areas. The results shown in Fig. 3 reveal that the altitude profiles for cases 2 and 3 are not that all that different either. Indeed, in both cases, altitude is reduced early during the flight to a value slightly above 500 ft, the value at which the switch to the final approach phase is made. It is conjectured that this early reduction in altitude helps to improve the lateral attenuation in the sound propagation to the side of the flight

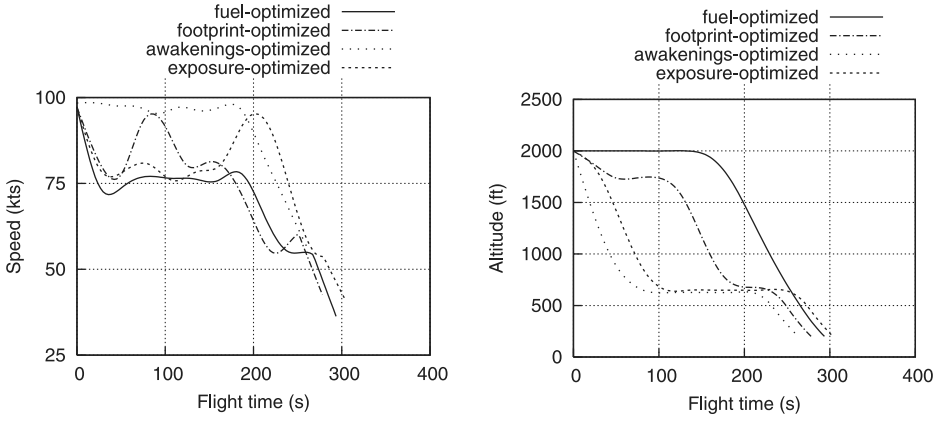

Fig. 3 Comparison of optimal SNI approach profiles.

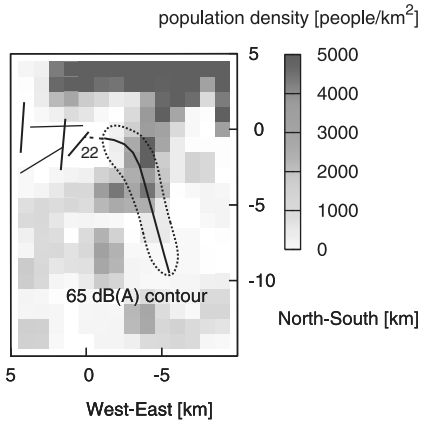

Case 1: *Fuel*-optimized solution

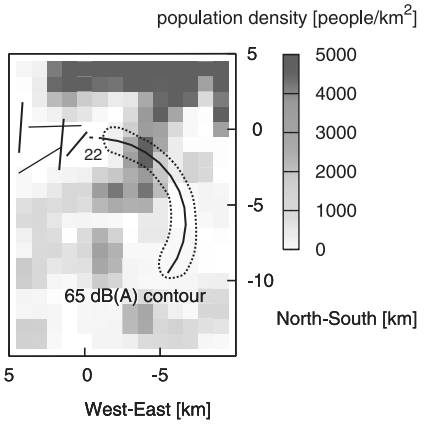

Case 2: *Awakenings*-optimized solution

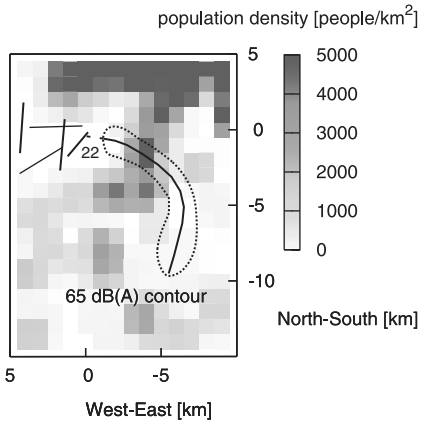

Case 3: *Exposure*-optimized solution

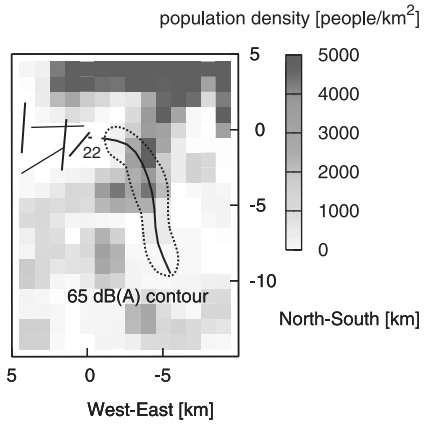

Case 4: *Footprint*-optimized solution

Fig. 4 Ground tracks of optimal approach trajectories, with underlying population and 65 dB contour shown.

path, which is a function of the elevation angle β_{elev} (see Fig. 5). The reason that the trajectory levels off at an altitude some 100 ft above the glide slope intercept altitude is related to the vertical deceleration constraint that has been imposed. The enforced deceleration constraint precludes a rapid change of flight-path angle to capture the glide slope path.

The results shown in Fig. 3 also bear out that the main difference between the case 2 and 3 solutions is that, in the exposure-optimized solution (case 3), airspeed is reduced early during the flight to a value of about 75 kts, whereas in the awakenings-optimized solution (case 2), speed is kept close to its initial value for the largest part of the flight.

In contrast to the solutions related to the site-specific criteria, the optimal trajectories associated to the generic (i.e., population distribution independent) criteria follow a more or less direct route from the initial point to the runway (see cases 1 and 4 in Fig. 4). The 65 dB(A) contours for the fuel-optimized (case 1) and footprint-optimized (case 4) solutions are located in relatively densely populated residential areas and, as a result, the number of people enclosed within the 65 dB(A) contour is significantly higher for the two generic cases relative to the site-specific criteria. The same holds true for the expected number of awakenings.

A close inspection of the results in Table 2 shows that the optimal value of the glide slope angle heavily depends on the (noise) criterion that has been specified. In particular for the Awakenings-optimized solution (case 2), the value of the glide slope angle turns out to be quite moderate (just slightly more than 5 deg).

A final observation relates to the fact that the exposure-optimized solution (case 3) features a rather complex trajectory, exhibiting frequent and large altitude/speed variations. Yet, the achieved reduction in footprint area size relative to the site-specific solutions remains rather modest.

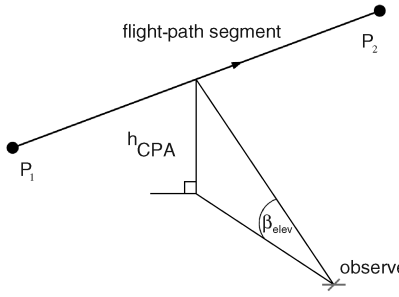

Fig. 5 Lateral attenuation geometry: a reduction in altitude at the closest point of approach (CPA) h_{CPA} leads to a reduction in elevation angle β_{elev}.

VII. Conclusions

In this paper, it has been demonstrated that the NOISHHH noise abatement trajectory optimization tool was successfully extended to include rotorcraft in addition to fixed-wing aircraft. The new rotorcraft-specific version of NOISHHH proved to be very useful in the discovery of the characteristic features of noise-optimized SNI instrument approach trajectories for helicopters. A parametric investigation brought to light that optimal trajectory behavior heavily depends on the specified environmental criteria. In particular, it was observed that the specification of a generic environmental criterion, such as minimum noise footprint area size, may result in trajectories that can actually inflict a significant noise impact to exposed communities in the vicinity of the flight path.

Results have been obtained for a limited number of hypothetical SNI procedure specifications only. Nevertheless, the NOISHHH tool proved to be very flexible in accommodating complex procedure specifications. This indicates that NOISHHH holds out great promise to be used as a design tool for future SNI approach procedures that enable low-noise terminal area operations.

Some of the observed results are somewhat surprising, such as the early descents and glide slope approaches that are relatively shallow. We believe this may be in part due to the assumptions made in the acoustic methodology underlying the INM 6.2 model (resulting, e.g., in excess lateral attenuation). A next step in the research will involve the implementation of noise models that more accurately capture the effects of maneuvering, wind, atmospheric conditions, and terrain features on the rotorcraft noise characteristics. Initially, an implementation of INM version 7.0 in NOISHHH is envisaged. Implementation of a higher fidelity noise model, such as the rotorcraft noise model [14] or the quasi-static acoustic mapping tool [3,4], is a longer term objective.

References

[1] Newman, D., and Wilkins, R., "Rotorcraft Integration into the Next Generation NAS," *Proc. of the American Helicopter Society (AHS) 54th Annual Forum*, American Helicopter Society, Alexandria, VA, May 1998.

[2] Haverdings, H., Van der Vorst, J., Gille, M., "Design and Execution of Piloted Simulation Tests of Steep Segmented and Curved Rotorcraft IFR Procedures at NLR," *Proceedings of the European Rotorcraft Forum*, National Aerospace Lab. Paper AO06, Sept. 2006.

[3] Atkins, E. M., and Xue, M., "Noise-Sensitive Final Approach Trajectory Optimization for Runway-Independent Aircraft," *Journal of Aerospace Computing, Information, and Communication*, Vol. 1, July 2004, pp. 269–287.
doi:10.2514/1.3924

[4] Xue, M., and Atkins, E. M., "Noise-Minimum Runway-Independent Aircraft Approach Design for Baltimore—Washington International Airport," *Journal of Aircraft*, Vol. 43, No. 1, 2006, pp. 39–51.
doi:10.2514/1.15692

[5] Vormer, F. J., Mulder, M., van Paassen, M. M., and Mulder, J. A., "Design and Preliminary Evaluation of Segment-based Routing Methodology," *Proceedings of AIAA Guidance, Navigation, and Control Conference* [CD-ROM], AIAA Paper 2002-4861 2002.

[6] Visser, H. G., and Wijnen, R. A. A., "Optimisation of Noise Abatement Arrival Trajectories," *The Aeronautical Journal*, Vol. 107, No. 1076, 2003, pp. 607–615.

[7] Visser, H. G., "Generic and Site-Specific Criteria in the Optimization of Noise Abatement Trajectories," *Transportation Research Part D: Transport and Environment*, Vol. 10, No. 5, 2005, pp. 405–419.
doi:10.1016/j.trd.2005.05.001

[8] Visser, H. G., and Wijnen, R. A. A., "Optimization of Noise Abatement Departure Trajectories," *Journal of Aircraft*, Vol. 38, No. 4, 2001, pp. 620–627.
doi:10.2514/2.2838

[9] Tang, S. F., "Optimization of Helicopter Noise Abatement Arrival Trajectories with the Software Tool NOISHHH," MSc Thesis, Delft Univ. of Technology, Delft, The Netherlands, 2007.

[10] Federal Aviation Administration, INM 6.0 Technical Manual, Office of Environment and Energy, Rept. FAA-AEE-02-01, 2002.

[11] Federal Aviation Administration, Policies and Procedures for Considering Environmental Impacts, Order 1050.1E, March 2006.

[12] Visser, H. G., "Optimization of Balanced Field Length Performance of Multi-Engine Helicopters," *Journal of Aircraft*, Vol. 37, July–Aug. 2000, pp. 598–605.
doi:10.2514/2.2671

[13] Zhao, Y., and Chen, R. T. N., "Critical Considerations for Helicopters During Runway Takeoffs," *Journal of Aircraft*, Vol. 32, July–Aug.1995, pp. 773–781.
doi:10.2514/3.46790

[14] Lucas, M. J., and Marcolini, M. A., "Rotorcraft Noise Model," *Proceedings of the American Helicopter Society Technical Specialists' Meeting for Rotorcraft Acoustics and Aerodynamics*, American Helicopter Society, Alexandria, VA, Oct. 1997, pp. 1–11.